Parametric Study on Pile-Soil Interaction Analyses By Overlaying Mesh Method

A. Ohta & F. Miura
Yamaguchi University, Japan

SUMMARY:
The overlaying mesh method (OMM) is an analytical approach that overlaps two or more independent different-sized-mesh models in the finite element analysis. In the OMM, detailed mesh model is used in the target area under consideration, with coarse mesh model elsewhere, in order to optimize calculation effort. In this study, we performed parametric study to investigate the accuracy of the analysis results by changing the mesh sizes, ground properties and pile characteristics in pile-ground interaction system.

Keywords: Finite Element Method, overlaying mesh method, pile-ground system

1. INTRODUCTION

The Overlaying mesh method (OMM) is an analytical approach that overlaps two or more independent different-sized-mesh models. In the OMM, detailed mesh model is used in elected area under consideration, with coarser mesh model elsewhere, in order to optimize calculation effort. In the previous study. (Belytchko et.al. 1990, p. 71) different size models are used to express a complex area with different material constants, but same type elements, such as two dimensional plane strain elements are used. In this research, we propose a new application method of the overlaying mesh method using different type elements such as beam elements and solid elements. We analyzed two types of pile foundation models using OMM, and proved that the proposed method is valid.

2. THEORY OF THE PROPOSED METHOD

2.1. Derivation of the fundamental equations for the OMM

In the OMM, two or more different-sized-mesh models are used, one is for modeling the wide area, which we call Global area, the other/others is/are used to model detailed area(s), which we call Local area(s), where we want to know the detailed behavior. In the soil-structure interaction problem, for example, the former is used to model the ground which widely extends, and the latter is used to model the structure of which shape is complex.

Let designate the Global area as Ω^G, the Local area as Ω^L and the boundary between these areas as Γ^{GL}. The image of the relationship of them is illustrated in Fig.1.

Displacement fields are independently defined in each Ω^G and Ω^L, i.e., u_i^G and u_i^L, respectively. The actual displacement u_i in Ω^L is defined as the sum of u_i^G and u_i^L, while u_i is equal to u_i^G outside the ΩL. Namely, the

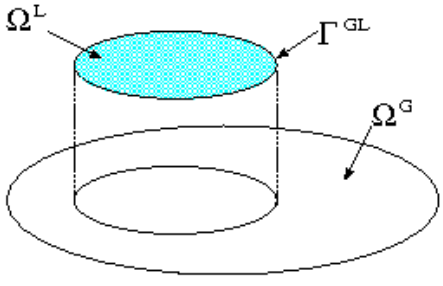

Figure 1. Superimposition of global and local areas

displacement u_i is defined as the following equations.

$$u_i = u_i^G + u_i^L \qquad \text{in} \quad \Omega^L \tag{2. 1}$$

$$u_i = u_i^G \qquad \text{in} \quad \Omega^G - \Omega^L \tag{2. 2}$$

To satisfy the continuity of the displacement at the boundary Γ^{GL}, the following condition is needed.

$$u_i^L = 0 \qquad \text{on} \quad \Gamma^{GL} \tag{2. 3}$$

Displacements u_i^G and u_i^L in Ω^G and Ω^L are expressed by using shape function matrices N^G and N^L and nodal displacement vectors $\overline{u_i^G}$ and $\overline{u_i^L}$ as follows.

$$u_i^G = N_{ij}^G \overline{u}_j^G \tag{2. 4}$$

$$u_i^L = N_{ij}^L \overline{u}_j^L \tag{2. 5}$$

By partially differentiating Eq. (2. 1) and using above equations, we obtain strain ε_{ij} as,

$$\varepsilon_{ij} = \varepsilon_{ij}^G + \varepsilon_{ij}^L \tag{2. 6}$$

In which

$$\varepsilon_{ij}^G = B_{ijk}^G \overline{u}_k^G \tag{2. 7}$$

$$\varepsilon_{ij}^L = B_{ijk}^L \overline{u}_k^L \tag{2. 8}$$

By using the principle of virtual work, we can obtain the next equation.

$$\int_\Omega \delta\varepsilon_{ij} D_{ijkl} \varepsilon_{kl} d\Omega = \int_\Omega \delta u_i b_i d\Omega + \int_\Gamma \delta u_i t_i d\Gamma \tag{2. 9}$$

Where, $\delta\varepsilon_{ij}$, δu_i , b_i, t_i, D_{ijkl} are virtual strain, virtual displacement, body force, surface traction and constitutive tensor, respectively. The left side of the equation stands for the virtual work due to the internal strains and the right side represents the virtual work done by the external forces. By substituting Eq. (2. 1), (2. 6), (2. 7) and (2. 8) into Eq. (2. 9), we can obtain the following equations.

$$\begin{aligned} &\int_\Omega \delta(\varepsilon_{ij}^G + \varepsilon_{ij}^L) D_{ijkl} (\varepsilon_{ij}^G + \varepsilon_{ij}^L) d\Omega \\ &= \int_\Omega \delta(u_i^G + u_i^L) b_i d\Omega + \int_\Gamma \delta(u_i^G + u_i^L) t_i d\Gamma \\ &\quad \int_\Omega (B_{ijm}^G \delta\overline{u}_m^G + B_{ijm}^L \delta\overline{u}_m^L) D_{ijkl} (B_{ijm}^G \overline{u}_m^G + B_{ijm}^L \overline{u}_m^L) d\Omega \end{aligned} \tag{2. 10}$$

$$= \int_\Omega (N_{ij}^G \delta u_i^G + N_{ij}^L \delta u_i^L) b_i d\Omega + \int_\Gamma (N_{ij}^G \delta u_i^G + N_{ij}^L \delta u_i^L) t_i d\Gamma \tag{2. 11}$$

By rewriting the above equations in the matrix form, we obtain the following equation.

$$\begin{bmatrix} K^G & K^{GL} \\ K^{LG} & K^L \end{bmatrix} \begin{Bmatrix} \bar{u}^G \\ \bar{u}^L \end{Bmatrix} = \begin{Bmatrix} \bar{f}^G \\ \bar{f}^L \end{Bmatrix} \tag{2. 12}$$

Where,

$$\begin{aligned} K^G &= \int_{\Omega^G} B_{ij}^G D_{ijkl} B_{kl}^G d\Omega^G \\ K^{GL} &= \int_{\Omega^L} B_{ij}^G D_{ijkl} B_{kl}^L d\Omega^L \\ K^{LG} &= \int_{\Omega^L} B_{ij}^L D_{ijkl} B_{kl}^G d\Omega^L \\ K^L &= \int_{\Omega^L} B_{ij}^L D_{ijkl} B_{kl}^L d\Omega^L \\ \bar{f}^G &= \int_{\Omega^G} N_i^G b_i d\Omega + \int_{\Gamma} N_i^G t_i d\Gamma \\ \bar{f}^L &= \int_{\Omega^L} N_i^L b_i d\Omega + \int_{\Gamma} N_i^L t_i d\Gamma \end{aligned} \tag{2. 13}$$

In which K^G and f^G are stiffness matrix and external force vector for the global area Ω^G, and K^L and f^L are stiffness matrix and external force vector for the local area Ω^L, respectively.

2.2 Linking the beam element and the plane strain solid element

According to the previous work, linkage matrices between global and local plane strain elements, K^{GL} and K^{LG}, are obtained from Eq. (2. 13). Linkage matrices between plane strain elements and beam elements, however, cannot be obtained in the same manner, because the strains are different between the beam element and the solid element. It is, therefore, necessary to develop a new method to link them.

The global nodal displacement at the same position as that of the local node, u'^G can be obtained by using the global shape function N^G and global nodal displacements $\bar{u}_k^G$ as Eq. (2. 14).

$$u_l'^G = N_{kl}^G \bar{u}_k^G \tag{2. 14}$$

Global strain at arbitrary point, ε^G, can be obtained from Eq. (2. 7), and also obtained using other element if the point is included inside the element and the coordinate of the nodal points of the element. Therefore, global strain can be obtained by using u'^G and local shape function B^L.

$$\begin{aligned} \varepsilon_{ij}^G &= B_{ijk}^G \bar{u}_k^G \\ &= B_{ijl}^L u_l'^G \end{aligned} \tag{2. 15}$$

Using Eq. (2. 14), we can obtain the following relationships.

$$\begin{aligned} B_{ijl}^L N_{kl}^G \bar{u}_k^G &= B_{ijl}^L u_l'^G \\ &= B_{ijk}^G \bar{u}_k^G \\ B_{ijk}^G &= B_{ijl}^L N_{kl}^G \end{aligned} \tag{2. 16}$$

Therefore, [K^{LG}]can be obtained as follows.

$$\begin{aligned}\left[K^{LG}\right] &= \int_{\Omega^L} B_{ij}^L D_{ijkl} B_{kl}^G d\Omega^L \\ &= \int_{\Omega^L} B_{ij}^L D_{ijkl} B_{klm}^L N_{mn}^G d\Omega^L \\ &= \int_{\Omega^L} B_{ij}^L D_{ijkl} B_{klm}^L d\Omega^L \cdot N_{mn}^G \\ &= \left[K^L\right]\left[N^G\right]\end{aligned} \tag{2. 17}$$

In the same manner, K^{GL} is expressed in the following way.

$$\left[K^{LG}\right] = \left[N^G\right]^T \left[K^L\right] \tag{2. 18}$$

2.3 Constitution of the local mesh

Figure 2 shows the total system which includes global model and local model. The local model contains beam elements of which area is designated by Ω^C. The local area modeled by solid elements is expressed by Ω^B and the global area by Ω^A. It is assumed that the areas Ω^A and Ω^C are not in contact. The constants of elasticity in the areas Ω^A and Ω^B are the same and expressed as D^1_{ijkl} and in the area Ω^C, D^1_{ijkl} in the global model and D^L_{ijkl} in the local model.

As for the boundaries, the boundary between Ω^A and Ω^B is designated by Γ^{AB}, in the same manner, the boundary between Ω^B and Ω^C is designated by Γ^{BC}. The boundary is divided into Γ^A, Γ^B and Γ^C according to the division of the areas Ω^A, Ω^B and Ω^C, respectively.

With the definitions above, K^G, K^L and K^{GL} are obtained as follows.

$$K^G = \int_{\Omega^A+\Omega^B+\Omega^C} B_{ij}^G D_{ijkl}^1 B_{kl}^G \, d\Omega \tag{2. 19}$$

$$K^L = \int_{\Omega^B} B_{ij}^L D_{ijkl}^1 B_{kl}^L d\Omega + \int_{\Omega^C} B_{ij}^L D_{ijkl}^L B_{kl}^L d\Omega \tag{2. 20}$$

$$K^{GL} = \int_{\Omega^B} B_{ij}^G D_{ijkl}^1 B_{kl}^L d\Omega + \int_{\Omega^C} B_{ij}^G D_{ijkl}^L B_{kl}^L d\Omega \tag{2. 21}$$

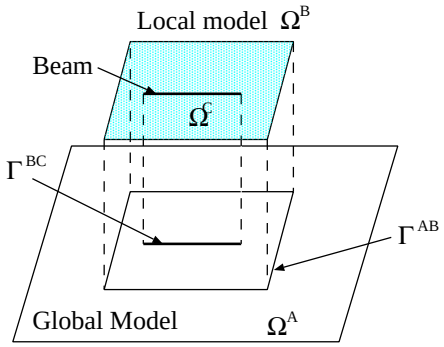

Figure 2. Superimposition of solid and beam elements

Equation (2. 10) can be written in the tensor form as;

$$\begin{aligned}&\int_{\Omega} \delta\varepsilon_{ij}^G D_{ijkl} \varepsilon_{kl}^G d\Omega + \int_{\Omega^L} \delta\varepsilon_{ij}^G D_{ijkl} \varepsilon_{kl}^L d\Omega^L \\ &+ \int_{\Omega^L} \delta\varepsilon_{ij}^L D_{ijkl} \varepsilon_{kl}^G d\Omega^L + \int_{\Omega^L} \delta\varepsilon_{ij}^L D_{ijkl} \varepsilon_{kl}^L d\Omega^L \\ &= \int_{\Omega} \delta u_i^G b_i d\Omega + \int_{\Omega^L} \delta u_i^L b_i d\Omega + \int_{\Gamma} \delta u_i^G t_i d\Gamma + \int_{\Gamma} \delta u_i^L t_i d\Gamma\end{aligned} \tag{2. 22}$$

The displacements, u_i, can be written in the following equation, in which symbols G, L, A, B and C stand for Global, Local and areas A, B and C.

$$u_i = \begin{cases} u_i^G = u_i^{GA} & \text{in} \quad \Omega^A \\ u_i^G + u_i^L = u_i^{GB} + u_i^{LB} & \text{in} \quad \Omega^B \\ u_i^G + u_i^L = u_i^{GC} + u_i^{LC} & \text{in} \quad \Omega^C \end{cases} \tag{2. 23}$$

As for the global displacement concerning the virtual displacement δu_i^G, and strain $\delta \varepsilon_{ij}^G$, we can obtain the following equation.

$$\begin{aligned} &\int_{\Omega^A} \delta\varepsilon_{ij}^{GA} D_{ijkl}^1 \varepsilon_{kl}^{GA} d\Omega + \int_{\Omega^B} \delta\varepsilon_{ij}^{GB} D_{ijkl}^1 \varepsilon_{kl}^{GB} d\Omega + \int_{\Omega^A} \delta\varepsilon_{ij}^{GC} D_{ijkl}^1 \varepsilon_{kl}^{GC} d\Omega \\ &\quad + \int_{\Omega^B} \delta\varepsilon_{ij}^{GB} D_{ijkl}^1 \varepsilon_{kl}^{LB} d\Omega \ + \int_{\Omega^C} \delta\varepsilon_{ij}^{GC} D_{ijkl}^L \varepsilon_{kl}^{LC} d\Omega \\ &= \int_{\Omega^A} \delta u_i^{GA} b_i d\Omega + \int_{\Omega^B} \delta u_i^{GB} b_i d\Omega + \int_{\Omega^C} \delta u_i^{GC} b_i d\Omega \\ &\quad + \int_{\Gamma} \delta u_i^{GA} t_i d\Gamma + \int_{\Gamma} \delta u_i^{GB} t_i d\Gamma + \int_{\Gamma} \delta u_i^{GC} t_i d\Gamma \end{aligned} \tag{2. 24}$$

By partially integrating the left part of Eq. (2. 24) using the Green's formula, the following equation is obtained.

$$\begin{aligned} &-\int_{\Omega^A} \left\{ D_{ijkl}^1 \varepsilon_{kl,l}^{GA} + b_i \right\} \delta u_i^{GA} d\Omega - \int_{\Omega^B} \left\{ D_{ijkl}^1 \left(\varepsilon_{kl,l}^{GB} + \varepsilon_{kl,l}^{LB} \right) + b_i \right\} \delta u_i^{GB} d\Omega \\ &-\int_{\Omega^C} \left\{ D_{ijkl}^1 \varepsilon_{kl,l}^{GC} + D_{ijkl}^L \varepsilon_{kl,l}^{LC} + b_i \right\} \delta u_i^{GC} d\Omega \ + \int_{\Gamma^A} \left(D_{ijkl}^1 \varepsilon_{kl}^{GA} n_j^A - t_i \right) \delta u_i^{GA} d\Gamma \\ &+\int_{\Gamma^B} \left\{ D_{ijkl}^1 \left(\varepsilon_{kl}^{GB} + \varepsilon_{kl}^{LB} \right) n_j^B - t_i \right\} \delta u_i^{GB} d\Gamma + \int_{\Gamma^C} \left\{ D_{ijkl}^1 \left(\varepsilon_{kl}^{GC} + \varepsilon_{kl}^{LC} \right) n_j^C - t_i \right\} \delta u_i^{GC} d\Gamma \\ &+\int_{\Gamma^{AB}} \left\{ D_{ijkl}^1 \varepsilon_{kl}^{GA} - D_{ijkl}^1 \left(\varepsilon_{kl}^{GB} + \varepsilon_{kl}^{LB} \right) \right\} n_j^B \delta u_i^{GAB} d\Gamma \\ &+\int_{\Gamma^{BC}} \left\{ D_{ijkl}^1 \left(\varepsilon_{kl}^{GB} + \varepsilon_{kl}^{LB} \right) - \left(D_{ijkl}^1 \varepsilon_{kl}^{GC} + D_{ijkl}^L \varepsilon_{kl}^{LC} \right) \right\} n_j^C \delta u_i^{GBC} d\Gamma = 0 \end{aligned} \tag{2. 25}$$

As the global displacements u_i^G is continuous in area Ω, the following relations can exist.

$$\delta u_i^{GA} = \delta u_i^{GB} = \delta u_i^{GAB} \quad \text{on} \quad \Gamma^{AB} \tag{2. 26}$$

$$\delta u_i^{GB} = \delta u_i^{GC} = \delta u_i^{GBC} \quad \text{on} \quad \Gamma^{BC} \tag{2. 27}$$

On the other hand, as for the local displacement concerning the virtual displacement δu_i^L, and strain $\delta \varepsilon_{ij}^L$, we can obtain the following equation.

$$\begin{aligned} &\int_{\Omega^B} \delta\varepsilon_{ij}^{LB} D_{ijkl}^1 \varepsilon_{kl}^{GB} d\Omega + \int_{\Omega^C} \delta\varepsilon_{ij}^{LC} D_{ijkl}^L \varepsilon_{kl}^{GC} d\Omega \\ &+\int_{\Omega^B} \delta\varepsilon_{ij}^{LB} D_{ijkl}^1 \varepsilon_{kl}^{LB} d\Omega + \int_{\Omega^C} \delta\varepsilon_{ij}^{LC} D_{ijkl}^L \varepsilon_{kl}^{LC} d\Omega \\ &= \int_{\Omega^B} \delta u_i^{LB} b_i d\Omega + \int_{\Omega^C} \delta u_i^{LC} b_i d\Omega + \int_{\Gamma^B} \delta u_i^{LB} t_i d\Gamma + \int_{\Gamma^C} \delta u_i^{LC} t_i d\Gamma \end{aligned} \tag{2. 28}$$

In the same manner as in the global area, Eq. (2. 28) can be written as,

$$
\begin{aligned}
&-\int_{\Omega^B}\left\{D^1_{ijkl}(\varepsilon^{GB}_{kl,l}+\varepsilon^{LB}_{kl,l})+b_i\right\}\delta u_i^{GB}d\Omega\\
&-\int_{\Omega^C}\left\{D^1_{ijkl}\varepsilon^{GC}_{kl,l}+D^L_{ijkl}\varepsilon^{LC}_{kl,l}+b_i\right\}\delta u_i^{GC}d\Omega\\
&+\int_{\Gamma^B}\left\{D^1_{ijkl}(\varepsilon^{GB}_{kl}+\varepsilon^{LB}_{kl})n_j^B-t_i\right\}\delta u_i^{GB}d\Gamma+\int_{\Gamma^C}\left\{(D^1_{ijkl}\varepsilon^{GC}_{kl}+D^L_{ijkl}\varepsilon^{LC}_{kl})n_j^C-t_i\right\}\delta u_i^{GC}d\Gamma \quad (2.29)\\
&+\int_{\Gamma^{AB}}\left\{D^1_{ijkl}\varepsilon^{GA}_{kl}-D^1_{ijkl}(\varepsilon^{GB}_{kl}+\varepsilon^{LB}_{kl})\right\}n_j^B\delta u_i^{GAB}d\Gamma\\
&+\int_{\Gamma^{BC}}\left\{D^1_{ijkl}(\varepsilon^{GB}_{kl}+\varepsilon^{LB}_{kl})-(D^1_{ijkl}\varepsilon^{GC}_{kl}+D^L_{ijkl}\varepsilon^{LC}_{kl})\right\}n_j^C\delta u_i^{GBC}d\Gamma=0
\end{aligned}
$$

And,

$$\delta u_i^{LB}=0 \quad \text{on} \quad \Gamma^{\mathrm{AB}} \tag{2.30}$$

In the Eq. (2. 25) and (2. 29), as the virtual displacements are arbitrary, we obtain the following equations.

$$D^1_{ijkl}\varepsilon^{GA}_{kl,l}+b_i=0 \qquad \text{in} \quad \Omega^A \tag{2.31}$$

$$D^1_{ijkl}(\varepsilon^{GB}_{kl,l}+\varepsilon^{LB}_{kl,l})+b_i=0 \qquad \text{in} \quad \Omega^B \tag{2.32}$$

$$D^1_{ijkl}\varepsilon^{GC}_{kl,l}+D^L_{ijkl}\varepsilon^{LC}_{kl,l}+b_i=0 \qquad \text{in} \quad \Omega^C \tag{2.33}$$

$$D^L_{ijkl}\varepsilon^{GC}_{kl,l}+D^L_{ijkl}\varepsilon^{LC}_{kl,l}+b_i=0 \qquad \text{in} \quad \Omega^C \tag{2.34}$$

$$D^1_{ijkl}\varepsilon^{GA}_{kl}n_j^A-t_i=0 \qquad \text{on} \quad \Gamma^A \tag{2.35}$$

$$D^1_{ijkl}(\varepsilon^{GB}_{kl}+\varepsilon^{LB}_{kl})n_j^B-t_i=0 \qquad \text{on} \quad \Gamma^B \tag{2.36}$$

$$(D^1_{ijkl}\varepsilon^{GC}_{kl}+D^L_{ijkl}\varepsilon^{LC}_{kl})n_j^C-t_i=0 \qquad \text{on} \quad \Gamma^C \tag{2.37}$$

$$(D^L_{ijkl}\varepsilon^{GC}_{kl}+D^L_{ijkl}\varepsilon^{LC}_{kl})n_j^C-t_i=0 \qquad \text{on} \quad \Gamma^C \tag{2.38}$$

$$\left\{D^1_{ijkl}\varepsilon^{GA}_{kl}-D^1_{ijkl}(\varepsilon^{GB}_{kl}+\varepsilon^{LB}_{kl})\right\}n_j^B=0 \qquad \text{on} \quad \Gamma^{AB} \tag{2.39}$$

$$\left\{D^1_{ijkl}(\varepsilon^{GB}_{kl}+\varepsilon^{LB}_{kl})-(D^1_{ijkl}\varepsilon^{GC}_{kl}+D^L_{ijkl}\varepsilon^{LC}_{kl})\right\}n_j^C=0 \qquad \text{on} \quad \Gamma^{BC} \tag{2.40}$$

$$\left\{D^1_{ijkl}(\varepsilon^{GB}_{kl}+\varepsilon^{LB}_{kl})-(D^L_{ijkl}\varepsilon^{GC}_{kl}+D^L_{ijkl}\varepsilon^{LC}_{kl})\right\}n_j^C=0 \qquad \text{on} \quad \Gamma^{BC} \tag{2.41}$$

By subtracting Eq. (2. 34) from Eq. (2. 33), Eq. (2. 38) from Eq. (2. 37), Eq. (2. 41) from Eq. (2. 40), we obtain Eq. (2. 42), (2. 43), (2. 44), respectively.

$$(D^1_{ijkl}-D^L_{ijkl})\varepsilon^{GC}_{kl,l}=0 \qquad \text{in} \quad \Omega^C \tag{2.42}$$

$$(D^1_{ijkl}-D^L_{ijkl})\varepsilon^{GC}_{kl}n_j^C=0 \quad \text{on} \quad \Gamma^C \tag{2.43}$$

$$(D^1_{ijkl}-D^L_{ijkl})\varepsilon^{GC}_{kl}n_j^C=0 \quad \text{on} \quad \Gamma^{BC} \tag{2.44}$$

From Eq. (2. 43) and (2. 44), equilibrium of stress is independently satisfied within the global model on the boundaries Γ^{BC} and Γ^{C}, and normal stress outward direction is 0. From Eq. (2. 42), (2. 43), (2. 44) we can get the next relationship.

$$(D^1_{ijkl}-D^L_{ijkl})\varepsilon^{GC}_{kl}=0 \qquad \text{in} \quad \Omega^C \tag{2.45}$$

This means that the stress of beam elements due to global model is 0 on the boundary of area Ω^C. And from Eq. (2. 45)

$$\varepsilon_{kl}^{GC} = 0 \qquad \text{in} \qquad \Omega^C \tag{2. 46}$$

Eq. (2. 33) and (2. 34) become

$$D_{ijkl}^{L}\varepsilon_{kl,l}^{LC} + b_i = 0 \qquad \text{in} \qquad \Omega^C \tag{2. 47}$$

In the same way, Eq. (2. 40) and (2. 41) become

$$\left\{D_{ijkl}^{1}(\varepsilon_{kl}^{GB} + \varepsilon_{kl}^{LB}) - D_{ijkl}^{L}\varepsilon_{kl}^{LC}\right\} n_j^B = 0 \qquad \text{on} \qquad \Gamma^{BC} \tag{2. 48}$$

This means that the stresses due to displacements in local model within area Ω^C on the boundary Γ^{BC}, equilibrium to those within area Ω^B. Stresses in the beam elements, therefore, can be expressed only by the local model and obtained only by the stiffness of the beam elements (Ohta et.al. 2007).

3. ANALYTICAL EXAMPLES

3.1 Vertical pile model

The vertical pile-footing-ground model used in this analysis is illustrated in Fig. 3. Ground and piles and footing are assumed to be elastic materials.

Young's modulus, sectional area, and moment inertia of the section of the pile are 200GPa, 0.2366×10^{-5}m^2, and 0.3940×10^{-5}m^4, respectively. Parameter of the plane elements are listed in Table3. 1.

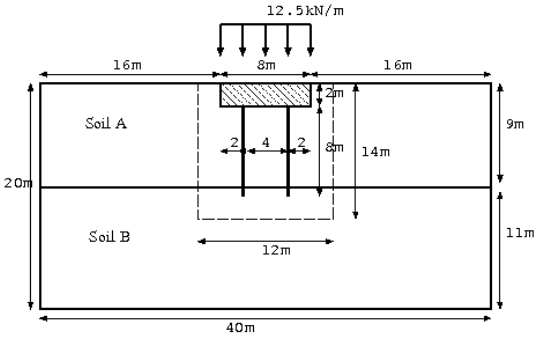

Figure 3. Vertical pile model

Finite element model with OMM is shown in Fig. 4. This model is divided into 800 global solid elements whose area is 1.0m^2, 16800 local solid elements whose area is 0.01m^2 and 160 local beam elements whose length is 0.1m(OMM FEM). To compare the accuracy, the ordinal finite mesh model(ordinal model) and coarse-mesh model(mesh 800) are also analysed. The ordinal finite mesh model is divided into 80000 solid elements whose area is 0.01m2 and 160 beam elements, the coarse-mesh model corresponds to the Global solid elements of the model shown in Fig.4.

Table 3.1. Parameter of the plane element

	Shearwave velocity(m/s)	Unit weight(kN/m^3)	Poisson's ration
Soil A	150	17	0.3
Soil B	450	17	0.3
Footing	1500	17	0.3

Numerical analysis results are compared in Fig. 5, 6 and 7. Horizontal placements of the beam elements are illustrated in Fig. 5, vertical displacements in Fig. 6 and rotational angles in Fig. 7. From these figures, it can be recognized that the differences of vertical response displacements between these models are very small but for the horizontal and rotational angle the differences are not so small.

The difference of the horizontal response displacements between the ordinal FEM and OMM FEM is about 0.1mm, and this is very small compared with the maximum response of the system of 2.9mm, in the vertical direction, the difference is about 0.03mm, while the maximum response is about 13.5mm. On the other hand, the differences of them between the ordinal FEM and mesh 800 are 0.02mm in horizontal direction and 0.08mm in vertical direction respectively, and they are about 4times of the differences between the ordinal FEM and OMM FEM. This means the validity of the proposed method. The distributions of the response displacements in the total system are shown in Fig. 8, 9, 10 and 11. From these figures the results are almost same in two models.

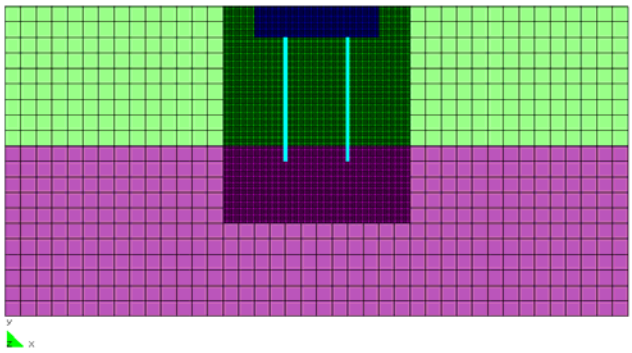

Figure 4. Finite element mesh of vertical piles with OMM

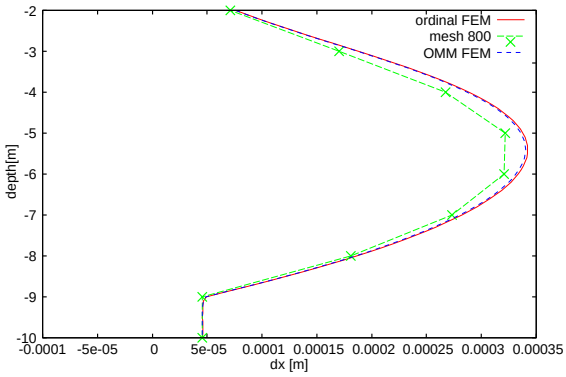

Figure 5. Comparison of horizontal displacements

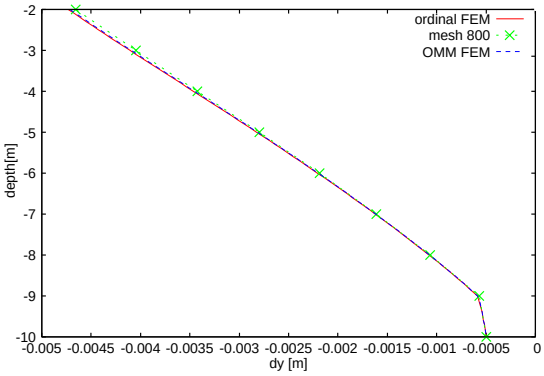

Figure 6. Comparison of vertical displacements

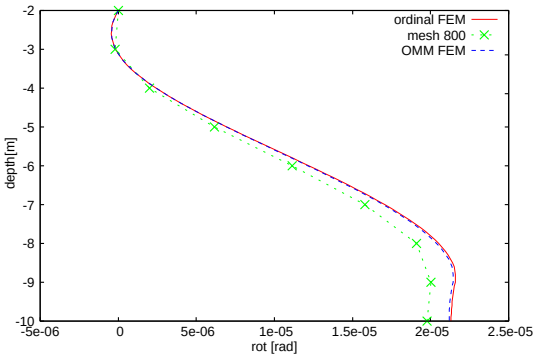

Figure 7. Comparison of rotational angle of pile

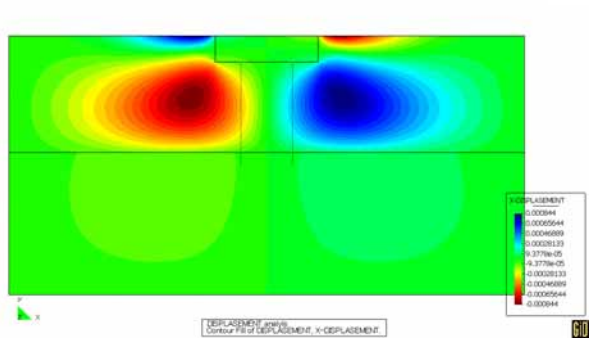

Figure 8. Distribution of horizontal displacement from normal finite element mesh

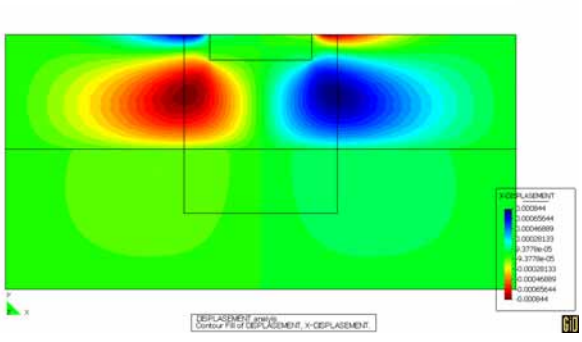

Figure 9. Distribution of horizontal displacement from finite element mesh with OMM

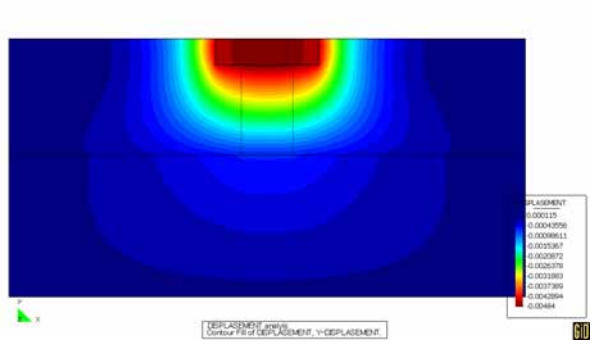

Figure 10. Distribution of vertical displacement from normal finite element mesh

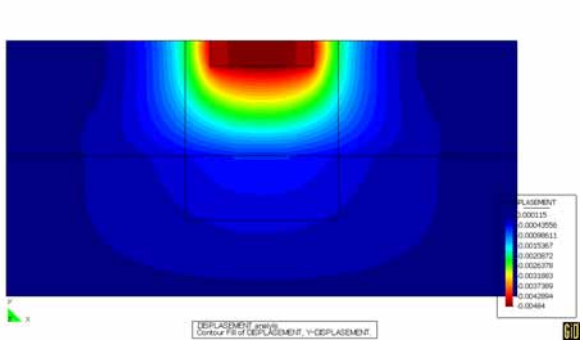

Figure 11. Distribution of vertical displacement from finite element mesh with OMM

3.2 Battered pile model

Figure 12 shows the battered pile-ground-footing model. The material constants are the same as those of the vertical pile models. Fig. 13 is OMM model. The OMM model is divided into 800 global solid elements whose area is 1.0m^2, 16960 local solid elements whose area is 0.01m^2 and 160 local beam elements. This model is called "OMMcase1". The ordinal model is divided into 80652 solid elements whose area is 0.01m^2 and 160 beam elements. This model us called "ordinal FEM". The mesh of the ordinal model is very complicated to express the battered piles, on the other hand, the mesh is very simple for the OMM model as shown in Fig. 13. Same global mesh as in the vertical pile is used for the OMM. In addition to these two models, two more models, "OMMcase2" and "OMMcase3" models were analysed. The size of global mesh of "OMM case2" and "OMM case3" is equal to the global mesh of "OMM case1" i.e. 1m. But the local mesh of "OMM case2" is 0.25m and coarser than that of "OMM case1"(0.1m), and the local mesh area of "OMM case3"(mesh size is 0.1m same as "OMM case1") is 6m and narrower than that of "OMM case1".

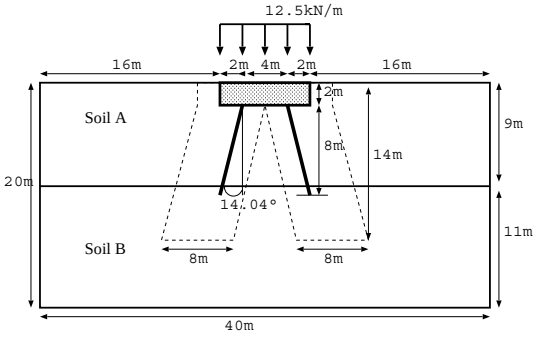

Figure 12. Battered pile model

The comparisons of horizontal and vertical displacements and rotational angle are made in Fig. 14, 15 and 16. In these figures, the differences between these models are little larger than those from the vertical piles model, especially for rotational angle.

The CPU time to analyze "ordinal FEM" and "OMMcase1" models are almost same in both cases. However, to generate the OMM is very easy, because we just put the battered piles models on the global model (ground model). This is a typical advantage of using OMM.

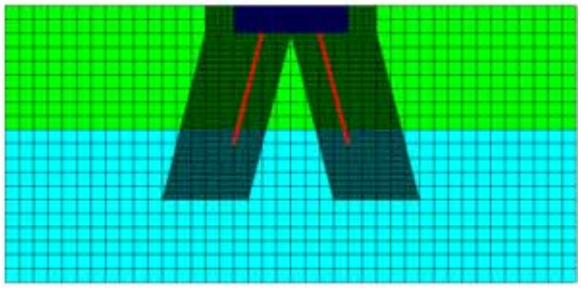

Figure 13. Finite element mesh of battered piles with OMM

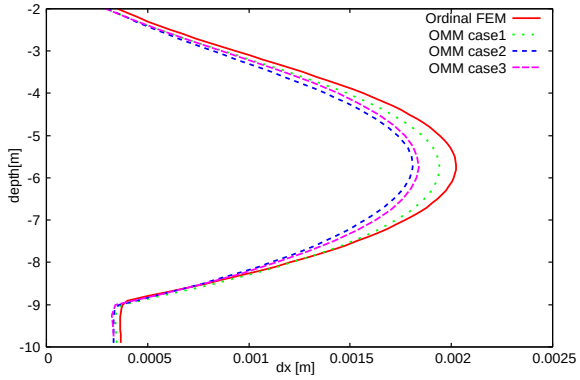

Figure 14. Comparison of horizontal displacements

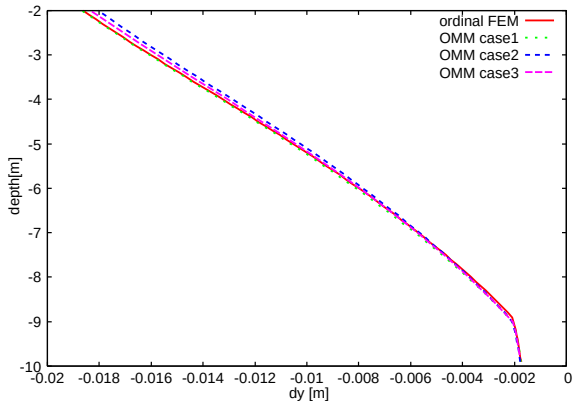

Figure 15. Comparison of vertical displacements

4. CONCLUSIONS

We derived the OMM in application of the soil-structure interaction system. Then we examined the validity of the method. For vertical pile model, we could get good agreement between the ordinal model and the OMM, but in the analysis of battered pile model, the difference is little larger than those for vertical pile models. We need to examine the reason and establish the better analysis method for the soil-structure interaction problem, and more we need to extend the method to three dimensional problem in which the advantage of the method will be remarkable.

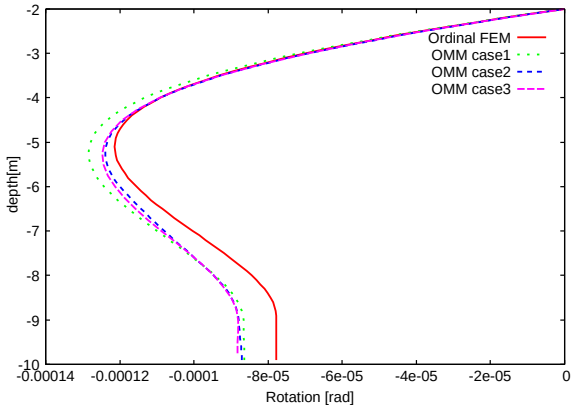

Figure 16. Comparison of rotational angle of pile

REFERENCES

T. Belytchko, J. Fish and A. Bayliss: The spectral overlay on finite elements for problems with high gradients, Computer methods in applied mechanics and engineering, **Vol.81** pp.71-89, 1990.

A. Ohta, Y. Ono, J. Kiyono and F. Miura: Finite element analysis of pile-soil interaction system by overlaying mesh method, 3rd Greece-Japan Workshop, 2007